Chemico-Biological Interactions 191 (2011) 199–205

Contents lists available at ScienceDirect

Chemico-Biological Interactions

journal homepage: www.elsevier.com/locate/chembioint

# Human and rodent aldo–keto reductases from the AKR1B subfamily and their specificity with retinaldehyde

F. Xavier Ruiz[a], Armando Moro[a], Oriol Gallego[a], Albert Ardèvol[b], Carme Rovira[b,c], J. Mark Petrash[d], Xavier Parés[a], Jaume Farrés[a,*]

[a] Department of Biochemistry and Molecular Biology, Universitat Autònoma de Barcelona, E-08193 Bellaterra, Barcelona, Spain
[b] Centre de Recerca en Química Teòrica, Parc Científic de Barcelona, Josep Samitier 1–5, E-08028 Barcelona, Spain
[c] Institució Catalana de Recerca i Estudis Avançats, Passeig Lluís Companys 23, E-08010 Barcelona, Spain
[d] Department of Ophthalmology, University of Colorado Denver, Aurora, CO 80045, United States

ARTICLE INFO

*Article history:*
Available online 15 February 2011

*Keywords:*
Aldo–keto reductases
Aldose reductase
Retinoic acid
Side-directed mutagenesis

ABSTRACT

NADP(H)-dependent cytosolic aldo–keto reductases (AKR) are mostly monomeric enzymes which fold into a typical $(\alpha/\beta)_8$-barrel structure. Substrate specificity and inhibitor selectivity are determined by interaction with residues located in three highly variable loops (A, B, and C). Based on sequence identity, AKR have been grouped into families, namely AKR1–AKR15, containing multiple subfamilies. Two human enzymes from the AKR1B subfamily (AKR1B1 and AKR1B10) are of special interest. AKR1B1 (aldose reductase) is related to secondary diabetic complications, while AKR1B10 is induced in cancer cells and is highly active with all-*trans*-retinaldehyde. Residues interacting with all-*trans*-retinaldehyde and differing between AKR1B1 and AKR1B10 are Leu125Lys and Val131Ala (loop A), Leu301Val, Ser303Gln, and Cys304Ser (loop C). Recently, we demonstrated the importance of Lys125 as a determinant of AKR1B10 specificity for retinoids. Residues 301 and 304 are also involved in interactions with substrates or inhibitors, and thus we checked their contribution to retinoid specificity. We also extended our study with retinoids to rodent members of the AKR1B subfamily: AKR1B3 (aldose reductase), AKR1B7 (mouse *vas deferens* protein), AKR1B8 (fibroblast-growth factor 1-regulated protein), and AKR1B9 (Chinese hamster ovary reductase), which were tested against all-*trans* isomers of retinaldehyde and retinol. All enzymes were active with retinaldehyde, but with $k_{cat}$ values (0.02–0.52 $min^{-1}$) much lower than that of AKR1B10 (27 $min^{-1}$). None of the enzymes showed oxidizing activity with retinol. Since these enzymes (except AKR1B3) have Lys125, other residues should account for retinaldehyde specificity. Here, by using site-directed mutagenesis and molecular modeling, we further delineate the contribution of residues 301 and 304. We demonstrate that besides Lys125, Ser304 is a major structural determinant for all-*trans*-retinaldehyde specificity of AKR1B10.



## 1. Introduction

Aldo–keto reductases (AKR) are monomeric NAD(P)H-dependent enzymes which fold into a typical $(\alpha/\beta)_8$-barrel structure. They catalyze the reduction of carbonyl compounds using a variety of physiological substrates, including lipids, steroids, catecholamines, prostaglandins and retinoids [1]. Based on cluster analysis, AKR enzymes have been grouped into fifteen different families, having less than 40% amino acid identity with any other family, while subfamilies may be defined by higher than 60% identity in amino acid sequence among subfamily members [2,3]. AKR1B subfamily includes human members 1B1 and 1B10 which have been widely studied. 1B1 (aldose reductase) is upregulated in hyperglycemia, reduces glucose to sorbitol and was consistently related with secondary diabetic complications [4]. 1B10 (aldose reductase-*like* or small intestine reductase) is highly active with all-*trans*-retinaldehyde [5], a crucial molecule in the retinoic acid synthesis pathway, and induced in different types of cancer [6–11]. Recently a novel human member, 1B15, never found at protein level, was predicted from genomic analysis [12,13]. The murine AKR1B subfamily has three well-characterized members: 1B3 (aldose reductase) [14], 1B7 (androgen-dependent *vas deferens* protein, MVDP) [15], and 1B8 (fibroblast-dependent growth factor 1, FR-1) [16]. While 1B3 is highly similar to 1B1 in terms of tissue distribution and kinetic properties, 1B7 and 1B8 present distinct patterns [12]. Much less is known about the rat enzymes and only some information is available for 1B4 [17]. Also characterized is 1B9, an inducible form expressed in

* Corresponding author at: Department of Biochemistry and Molecular Biology, Universitat Autònoma de Barcelona, E-08193 Bellaterra, Barcelona, Spain.
Tel.: +34 93 5812557; fax: +34 93 5811264.
*E-mail address:* jaume.farres@uab.es (J. Farrés).

0009-2797/$ – see front matter © 2011 Elsevier Ireland Ltd. All rights reserved.
doi:10.1016/j.cbi.2011.02.007

Chinese hamster ovary cells [18]. While sequence identity between members of the AKR1B subfamily belonging to different species is high (70–84%), it remains to be investigated whether the retinoid specificity of 1B10 is shared by other members of this subfamily.

Previously we characterized the three-dimensional structure of a ternary complex of 1B10 with cofactor and inhibitor tolrestat and provided the basis for its high all-*trans*-retinaldehyde reductase activity [9,19]. Important differences were observed between the substrate-binding pockets of 1B1 and 1B10, which were predicted by molecular dynamics simulations and confirmed by site-directed mutagenesis. The structural features making 1B10 highly efficient for all-*trans*-retinaldehyde were localized in the external part of the substrate-binding site, including position 125.

Here we performed computer search to identify novel functional genes from the AKR1B subfamily and report kinetic studies on rodent members of the AKR1B subfamily (1B3, 1B7, 1B8, and 1B9) with retinoids. Moreover, we further studied the structural determinants of high all-*trans*-retinaldehyde reductase activity of human 1B10 by site-directed mutagenesis and molecular dynamics of the retinoid-binding site. Results clearly show that residue 304, in addition to residue 125, is critical for efficient retinoid catalysis.

## 2. Materials and methods

### 2.1. Sequence and phylogenetic analyses of the AKR1B subfamily

Homology between *AKR1B* genes was analyzed using Homologene (http://www.ncbi.nlm.nih.gov/homologene). In addition, the UniGene database was checked to identify mRNA and EST of the newly identified open reading frames. Phylogeny analysis was performed as reported [20]. Multiple amino acid sequence alignments were performed using the Clustal W program [21].

### 2.2. Site-directed mutagenesis

K125L, V301A, V301L, V301F, V301N and S304C single mutants were obtained using the wild-type AKR1B10 cDNA cloned into pET30-Xa/LIC as a template. Based on the Quickchange™ Site-Directed Mutagenesis Kit method (Stratagene), we designed two primers for each mutation as follows:

| AKR1B10 mutant | Primer | Sequence | Amino acid positions |
|---|---|---|---|
| K125L | *Forward* | 5′-GGATGACCTTTTCCCC***CT***AGATGATAAAGGTAATGCC-3′ | 120–131 |
| | *Reverse* | 5′-ATTACCTTTATCATCT***AG***GGGGAAAAGGTCATCCCCAG-3′ | 118–130 |
| V301A | *Forward* | 5′-CCTGTAACG***C***GTTGCAATCCTC-3′ | 298–305 |
| | *Reverse* | 5′-GATTGCAAC***G***CGTTACAGGCC-3′ | 297–304 |
| V301L | *Forward* | 5′-GCCTGTAAC***C***TGTTGCAATCC-3′ | 298–304 |
| | *Reverse* | 5′-ATTGCAACA***G***GTTACAGGCCC-3′ | 297–303 |
| V301F | *Forward* | 5′-GGGCCTGTAAC***TT***CTTGCAATCCTCTC-3′ | 297–306 |
| | *Reverse* | 5′-GAGGATTGCAAG***AAG***TTACAGGCCCTC-3′ | 297–305 |
| V301N | *Forward* | 5′-GGGCCTGTAAC***AAC***TTGCAATCCTCTC-3′ | 297–306 |
| | *Reverse* | 5′-GAGGATTGCAAG***TTG***TTACAGGCCCTC-3′ | 297–305 |
| S304C | *Forward* | 5′-TGTAACGTGTTGCAAT***G***CTCTCATTTGGAAGACTATC-3′ | 299–310 |
| | *Reverse* | 5′-GTCTTCCAAATGAGAG***C***ATTGCAACACGTTACAGGCC-3′ | 298–309 |

Mutated nucleotides are highlighted in bold and italics. K125L/S304C double mutant was prepared with pET30-Xa/LIC-AKR1B10 S304C as a template, by using the primers for K125L mutation. All reactions were performed in a DNA thermal cycler (MJ Research) with *Pfu Turbo* DNA Polymerase (Stratagene). PCR products were incubated with *Dpn*I at 37 °C for 60 min. This treatment ensured the digestion of the *dam*-methylated parental strand. The resulting nicked-circular mutagenic strands were transformed into *Escherichia coli* BL21. DNA sequences were verified to ensure that unwanted mutations were absent.

### 2.3. Cloning, expression and purification of AKR1B enzymes

1B3 and 1B8 were cloned, expressed and purified as described previously [22]. 1B7 cDNA sequence was obtained from the Mammalian Gene Collection (MGC) clones provided by LGC Promochem (MGC:107658 IMAGE:6775941). 1B1, 1B7, 1B9, 1B10 and all 1B10 mutants were cloned, expressed and purified as described previously [5,19]. Briefly, *E. coli* BL21 strain transformed with the plasmid pET16b (or pET30-Xa/LIC for 1B7 and the mutants), encoding each protein with an N-terminal $His_{10}$ tag ($His_6$ tag for the mutants), was grown in 2 × YT medium at 23 °C for 8 h. Protein expression was induced by the addition of 1 mM isopropyl-1-thio-β-D-galactopyranoside (IPTG, Sigma–Aldrich). Proteins were purified using a nickel-charged chelating Sepharose® Fast Flow resin (GE Healthcare). The enzymes were eluted by a 0.06–1.0 M imidazole (Sigma–Aldrich) gradient in 50 mM Tris–HCl, 100 mM NaCl, pH 8.0. Fractions containing AKR were collected and dialyzed twice against 10 mM sodium phosphate, 1 mM EDTA, pH 8.0.

### 2.4. Enzyme kinetics

Standard activities were measured prior to each kinetic experiment by using D,L-glyceraldehyde as a substrate [23]. Activity with retinoids was performed as reported [5,19]. Kinetic constants were expressed as the mean ± SEM of at least three independent determinations.

### 2.5. Molecular dynamics simulations

The initial structures for the simulations were obtained from docking of the substrate into the binding cavity, as described [19]. The Cornell et al. force-field [24], as implemented in AMBER 7.0 program [25], was used. All-*trans*-retinaldehyde and the cofactor were parameterized by using the antechamber module of AMBER. The system was equilibrated in several steps. First, all water molecules and counterions were relaxed with a gradient minimizer, and then the whole system was equilibrated. Next, the system was equilibrated at 100 K (50 ps), 200 K (25 ps), and 300 K (25 ps), coupling a bath to achieve the desired temperature. The simulations were continued for 4–10 ns, depending on the protein mutant, at constant pressure and temperature. The average structure, during the last nanosecond was taken for analysis.

## 3. Results and discussion

### 3.1. In silico analysis of human and rodent AKR1B genes and gene products

Fig. 1 depicts the genome organization of the *AKR1B* gene cluster in human, mouse and rat species. Human *AKR1B* genes are tandemly arrayed on chromosome 7q33–35, indicating that they

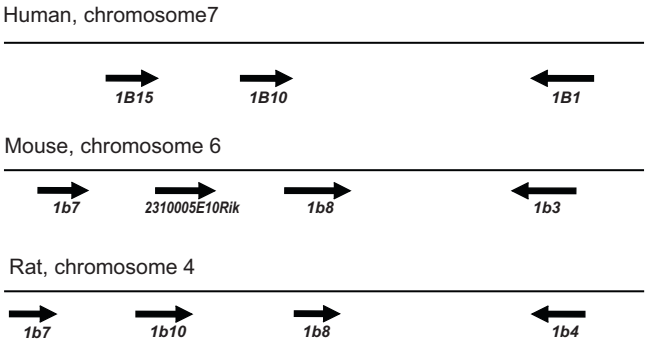


**Fig. 1.** Genomic organization of human and rodent *AKR1B* genes in syntenic regions. Arrows indicate relative gene size and the direction of transcription.
Adapted from HomoloGene database at National Center for Biotechnology Information (http://www.ncbi.nlm.nih.gov/homologene).

likely originated from ancient duplication events [12,13]. Syntenic regions in mouse and rat genomes, also including additional flanking genes, are found in chromosomes 6 and 4, respectively. Human genome includes three paralogous genes (namely *1B1*, *1B10* and *1B15*), while four genes are found in each murine (*1b3*, *1b7*, *1b8*, and *2310005E10Rik*) and rat (*1b4*, *1b7*, *1b8*, and *1b10*) genomes. Some of them are known functional genes, while others are predicted on the basis of sequence homology and exon–intron structure. Each gene consists of 10 exons. The direction of transcription is conserved for all the *AKR1B* genes among the three species. Transcription occurs from the opposite strand in *1B1*, *1b3* and *1b4* genes, suggesting an ancient inversion event which likely predated the *1B10/1B15* duplication in view of the percentage of sequence identity, as mentioned below.

Table 1 lists *AKR1B* genes and their corresponding gene products, with the currently accepted nomenclatures according to the NCBI and AKR (http://www.med.upenn.edu/akr) homepages. The gene product of *locus tcag7.1260*, also known as *LOC441282*, was recently named AKR1B15 (http://www.genenames.org/data/hgnc_data.php?match=AKR1B15), after having evidence that it is a functional gene. The encoded protein showed 92% and 67% amino acid identity with 1B10 and 1B1, respectively. This would suggest a very recent duplicatory event between *1B10* and *1B15* genes and a closely related biological function. A *RIKEN cDNA 2310005E10* gene from mouse and *Akr1b10* gene from rat (both cDNAs were found in EST libraries) have also been included and, while a definitive classification is pending, we propose the corresponding proteins to be named AKR1B16 and AKR1B17 (currently known as rat AKR1B10 [26]), respectively, while awaiting for the designation assignment by the AKR homepage.

Based on sequence identities and multiple alignments, an unrooted phylogenetic tree was constructed, using chicken 1B12 as an outgroup (Fig. 2). Analysis shows twelve proteins from human and rodents grouped in at least four different clusters which are labeled after representative enzymes from each group, namely, aldose reductase, small intestine reductase, AKR1B7 type and AKR1B8 type. As expected, all aldose reductases appear in a single cluster, well differentiated from the remaining AKR1B members. Chinese hamster 1B9 and rat 1B13 cluster with mouse 1B8 and thus they could be considered orthologous proteins. Rat 1B14 clusters together with mouse 1B7, and rat 1B17 clusters with mouse 1B16, suggesting that they are pairwise orthologous.

On the basis of genomic structure, sequence identity, phylogenetic analysis and enzymatic activity with glucose [14,27], human *1B1*, mouse *1b3* and rat *1b4* are clearly orthologous genes coding for aldose reductase, although differences exist in the level and pattern of expression, and activity between these species [22,28].

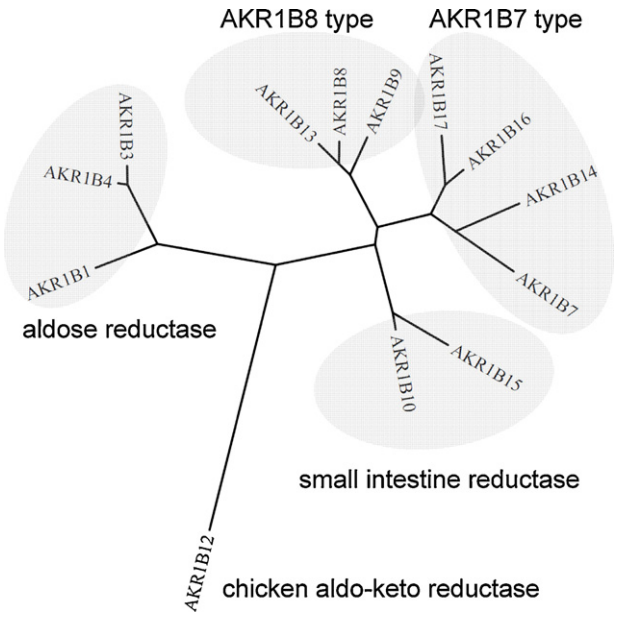


**Fig. 2.** Unrooted phylogenetic tree of AKR1B proteins. Different clusters are indicated by shaded ovals. Data were obtained by using PhyML, for multiple alignment, and TreeDyn to build a radial dendrogram, from the site (http://www.phylogeny.fr/phylo_cgi/express.cgi). Chicken AKR1B12 was used as an outgroup.

In contrast, human *1B10* gene orthologs cannot be unambigously assigned at this time. Based on sequence identity, tissue distribution and catalytic properties of their gene products [29], neither *1b7* nor *1b8* seems to be the true ortholog of the *1B10* gene. Mouse 1B7 protein has very low enzymatic activity and limited tissue distribution (mostly present in adrenal gland) [30,31]. Mouse 1B8 has very similar catalytic properties to human 1B1 and it is induced by fibroblast growth factor while 1B10 is not; however, in contrast to 1B1, 1B8 has a higher $K_m$ for D,L-glyceraldehyde and lacks activity with glucose [28]. While awaiting enzymatic characterization, 1B15 orthologs cannot be unambiguosly assigned either.

We also performed a multiple alignment of amino acid sequences from AKR1B enzymes, including only residues within variable loops A, B and C, which are highly variable regions providing substrate specificity (Fig. 3). Taking into account important residues for retinaldehyde binding in 1B10 [19], we then looked at non-conserved residues between aldose reductases and 1B10. The following substitutions were observed: K/L125 and A/V131 in loop A, and V/L301, Q/S303 and S/C304 in loop C (Figs. 3 and 4). It is noteworthy that Lys125, not present in aldose reductases, was shared by many other AKR1B members. Val301 was only found in 1B10 and chicken 1B12. The role of residues 125 and 301 in retinoid specificity was examined in a previous work [19], and the presence of Lys125 appeared to be an important determinant for all-*trans*-retinaldehyde specificity. Here we will further investigate the role of residue 301 and, for the first time, that of residue 304.

### 3.2. Comparison of kinetic constants between AKR1B enzymes

We cloned, expressed and purified human 1B1 and 1B10, murine 1B3, 1B7 and 1B8, and Chinese hamster 1B9. In Table 2, we compare their kinetic properties with retinoids, including recently published data for rat 1B13 [32], 1B14 [33] and 1B17 [26]. All the enzymes showed similar $k_{cat}$ values with glyceraldehyde (~30 $min^{-1}$), with the exception of 1B7, 1B14 and 1B17, which usually displayed lower $k_{cat}$ values with all the substrates [22,26]. 1B1 and 1B3 behaved as typical aldose reductases, having low $K_m$ values for glyceraldehyde (~50 μM) and low activity with retinaldehyde. The remaining

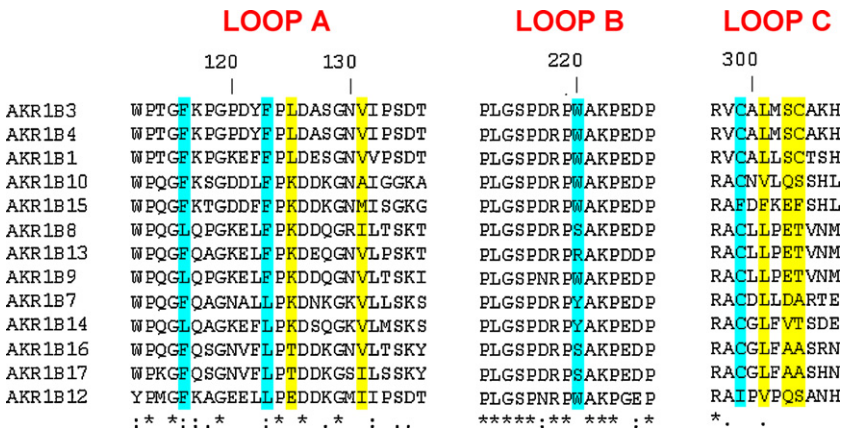


**Fig. 3.** Alignment of AKR1B sequences showing residues within variable loops A, B and C. Sequences were aligned by using the Clustal W program [21]. Important residues for retinaldehyde binding in AKR1B10 are highlighted: in blue, conserved residues between aldose reductases and AKR1B10. In yellow, non-conserved residues. Sequence identities are indicated by asterisks (*), conservative substitutions by colons (:) and semi-conservative substitutions by dots (.). (For interpretation of the references to color in this figure legend, the reader is referred to the web version of the article.)

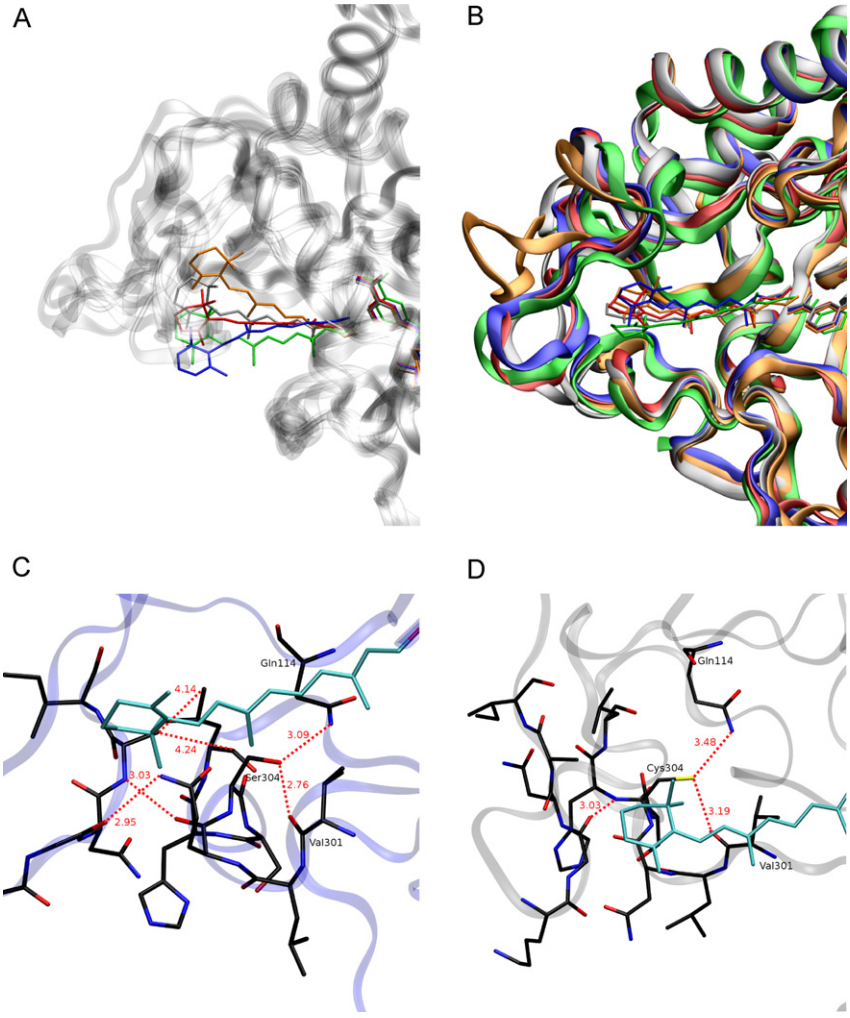


**Fig. 4.** Molecular dynamics of 1B1, 1B10 and 1B10 mutants complexed with all-*trans*-retinaldehyde. Average structures of five different computer simulations, with extensive calculation times between 4 and 10 ns, were obtained during the last 1 ns of each simulation. Panels A and B show different views of superimposed structures. In A, slightly different substrate conformations are highlighted. In B, loop A motion is quite different in the double mutant in comparison with other structures. Main chain is represented as a ribbon while all-*trans*-retinaldehyde and $NADP^+$ molecules are represented by sticks. Color codes: 1B10 (blue), K125L (red), S304C (gray), K125L/S304C (orange), and AKR1B1 (green). Panels C and D show details of the interactions around residue 304 in wild-type 1B10 (C) and 1B10 S304C mutant (D), including bound all-*trans*-retinaldehyde (cyan). Atomic distances (Å) between amino acid side chains are shown in red. (For interpretation of the references to color in this figure legend, the reader is referred to the web version of the article.)

**Table 1**
Percentage of amino acid sequence identity between AKR1B enzymes from human, rodents and chicken.

| | NCBI | AKR | Sequence identity (%) | | |
|---|---|---|---|---|---|
| | | | 1B1 | 1B10 | 1B15 |
| Human | | | | | |
| Aldose reductase | *AKR1B1* | 1B1 | – | 71 | 67 |
| Small intestine reductase | *AKR1B10* | 1B10 | 71 | – | 92 |
| | *AKR1B15* | 1B15 | 67 | 92 | – |
| Mouse | | | | | |
| Aldose reductase | *Akr1b3* | 1B3 | 86 | 71 | 68 |
| Mouse *vas deferens* | *Akr1b7* | 1B7 | 71 | 78 | 77 |
| FGF-induced protein | *Akr1b8* | 1B8 | 70 | 83 | 80 |
| | *2310005E10Rik* | 1B16* | 70 | 83 | 80 |
| Rat | | | | | |
| Aldose reductase | *Akr1b4* | 1B4 | 86 | 71 | 68 |
| | *Akr1b7* | 1B14 | 69 | 78 | 77 |
| | *Akr1b8* | 1B13 | 70 | 82 | 81 |
| | *Akr1b10* | 1B17* | 70 | 83 | 80 |
| Hamster | | | | | |
| CHO reductase | *CGU81045* | 1B9 | 71 | 84 | 82 |
| Chicken | | | | | |
| Chicken aldo–keto reductase | *AJ295030* | 1B12 | 67 | 70 | 67 |

* indicates proposed nomenclature.

AKR1B enzymes displayed millimolar (0.1–8.0 mM) $K_m$ values for glyceraldehyde and very low or no activity (1B13 and 1B14) with retinaldehyde, except 1B10, which reached a $k_{cat}$ value comparable to that with glyceraldehyde. Neither mouse 1B8 nor their likely orthologs in rat (1B13) and Chinese hamster (1B9) show great activity with retinaldehyde. Thus, human 1B10 is, so far, the only AKR1B with a high $k_{cat}$ value for retinaldehyde reduction. None of the examined enzymes, except for 1B10, showed oxidizing activity with retinol.

In a previous work [19], the presence of Lys125 in 1B10 appeared to be the main determinant for all-*trans*-retinaldehyde specificity. Remarkably, most 1B enzymes contain a Lys residue at position 125, except for 1B16 and 1B17 (with Thr), and aldose reductases (with Leu). In view of the present kinetic results, we must conclude that Lys125 is not the only structural determinant for high retinaldehyde reductase activity, and thus other residues should contribute to retinaldehyde specificity.

### 3.3. Kinetic constants of single and double mutants of AKR1B10

As mentioned above, residues 301 and 304, located in loop C, differ between 1B1 and 1B10 and recently, along with residues 114, 125 and 303, have been implicated in selective inhibitor binding between these two enzymes [34–37]. Previously we had shown that the V301L mutation, which mimics the 1B1 structure, had a moderate effect on the kinetic constants of 1B10. In addition, the double mutation K125L/V301L did not improve retinoid specificity with regard to the single K125L mutant [19]. Here we investigated the effect of substituting Val301 of 1B10 with residues having different molecular size and polarity (Table 3). No changes in kinetics with glyceraldehyde were observed, which reflects the fact that residue 301 is located in the most external part of the substrate-binding site, far away from where a small molecule, such as glyceraldehyde, interacts. Regarding the kinetics with retinaldehyde isomers: $K_m$ values did not vary much, while by increasing residue volume there was a corresponding decrease in the $k_{cat}$ values, the Leu effect being intermediate between that of Ala and Phe. On the other hand, the higher polarity incorporated by the V301N mutation might also have contributed to the large $k_{cat}$ decrease observed for this mutant. These data emphasize the importance of the molecular size and polarity of the residues in the substrate/inhibitor binding site of 1B1 and 1B10, which may account for their different substrate and inhibitor properties [36].

**Table 2**
Kinetic constants of human and rodent AKR1B enzymes.

| Substrate | Aldose reductase | | AKR1B7 type | | | AKR1B8 type | | | 1B10 |
|---|---|---|---|---|---|---|---|---|---|
| | 1B1 | 1B3 | 1B7 | 1B14[a] | 1B17[b] | 1B8 | 1B13[c] | 1B9 | |
| D,L-Glyceraldehyde | | | | | | | | | |
| $K_m$ | 0.05 ± 0.01 | 0.04 ± 0.01 | 8.0 ± 0.9 | 0.12 | 0.096 | 0.3 ± 0.06 | 2 | 3.5 ± 0.5 | 5.7 ± 0.8 |
| $k_{cat}$ | 31 ± 1 | 31 ± 1 | 4.5 ± 0.1 | 1.4 | 3 | 20 ± 0.6 | 35 | 36 ± 1 | 35 ± 1 |
| $k_{cat}/K_m$ | 660 ± 80 | 720 ± 85 | 0.6 ± 0.1 | 11.7 | 31 | 68 ± 14 | 17 | 10.5 ± 1.5 | 6.2 ± 0.9 |
| All-*trans*-retinaldehyde | | | | | | | | | |
| $K_m$ | 1.1 ± 0.1 | 1.0 ± 0.1 | 0.5 ± 0.1 | | 2.6 | 2.1 ± 0.5 | | 2.0 ± 0.2 | 0.6 ± 0.1 |
| $k_{cat}$ | 0.35 ± 0.01 | 0.52 ± 0.02 | 0.02 ± 0.01 | N.A. | 0.58 | 0.05 ± 0.01 | N.A. | 0.27 ± 0.01 | 27 ± 1 |
| $k_{cat}/K_m$ | 320 ± 30 | 540 ± 90 | 42 ± 6 | | 220 | 22 ± 6 | | 140 ± 18 | 45,000 ± 7600 |
| All-*trans*-retinol | | | | | | | | | |
| $K_m$ | | | | | | | | | 0.4 ± 0.1 |
| $k_{cat}$ | N.A. | N.A. | N.D. | N.D. | N.D. | N.A. | N.D. | N.A. | 4.3 ± 0.3 |
| $k_{cat}/K_m$ | | | | | | | | | 12,300 ± 3600 |

Enzymes are grouped according to the clusters defined by phylogenetic analysis as depicted in Fig. 2. Units: $K_m$ (mM with D,L-glyceraldehyde, μM with retinoids), $k_{cat}$ ($min^{-1}$), $k_{cat}/K_m$ ($mM^{-1}$ $min^{-1}$). Activities were determined in 0.1 M sodium phosphate, pH 7.5, 0.2 mM NADPH, 25 °C, with D,L-glyceraldehyde, and in 90 mM $KH_2PO_4$, 40 mM KCl, pH 7.4, 0.5 mM NADP/H, 37 °C, with retinoids, N.A., no activity; N.D., not determined.

[a] Data taken from [33].
[b] Data taken from [26].
[c] Data taken from [32].

**Table 3**
Kinetic constants of AKR1B10 and AKR1B10 V301 mutants.

| Substrate | 1B10 | V301A | V301L | V301F | V301 N |
|---|---|---|---|---|---|
| D,L-Glyceraldehyde | | | | | |
| $K_m$ | 5.7 ± 0.8 | 5.7 ± 0.6 | 6.0 ± 0.7 | 5.7 ± 0.6 | 5.4 ± 0.8 |
| $k_{cat}$ | 35 ± 1 | 37 ± 1 | 41 ± 1 | 36 ± 1 | 41 ± 2 |
| $k_{cat}/K_m$ | 6.2 ± 0.9 | 6.6 ± 0.7 | 7.0 ± 1 | 6.3 ± 0.7 | 7.5 ± 1.2 |
| All-*trans*-retinaldehyde | | | | | |
| $K_m$ | 0.6 ± 0.1 | 0.7 ± 0.1 | 0.6 ± 0.1 | 0.4 ± 0.1 | 0.4 ± 0.1 |
| $k_{cat}$ | 27 ± 1 | 10.9 ± 0.4 | 7.7 ± 0.3 | 6.6 ± 0.4 | 3.0 ± 0.1 |
| $k_{cat}/K_m$ | 45,000 ± 7600 | 15,600 ± 2000 | 12,700 ± 1400 | 17,900 ± 1700 | 8400 ± 1500 |

Units: $K_m$ (mM with D,L-glyceraldehyde, μM with retinoids), $k_{cat}$ ($min^{-1}$), $k_{cat}/K_m$ ($mM^{-1}$ $min^{-1}$). Activities were determined as in Table 2.

**Table 4**
Kinetic constants of AKR1B10, AKR1B10 K125L and S304C mutants, and AKR1B1.

| Substrate | 1B10 | K125L | S304C | K125L/S304C | 1B1 |
|---|---|---|---|---|---|
| D,L-Glyceraldehyde | | | | | |
| $K_m$ | 5.7 ± 0.8 | 5.2 ± 0.8 | 5.2 ± 0.6 | 2.6 ± 0.6 | 0.05 ± 0.01 |
| $k_{cat}$ | 35 ± 1 | 35.6 ± 0.1 | 29 ± 1 | 28 ± 1 | 31 ± 1 |
| $k_{cat}/K_m$ | 6.2 ± 0.9 | 7.0 ± 1 | 6.9 ± 0.9 | 10.8 ± 2.5 | 660 ± 80 |
| All-*trans*-retinaldehyde | | | | | |
| $K_m$ | 0.6 ± 0.1 | 0.15 ± 0.02 | 0.82 ± 0.08 | 0.9 ± 0.1 | 1.1 ± 0.1 |
| $k_{cat}$ | 27 ± 1 | 2.0 ± 0.1 | 2.0 ± 0.1 | 0.12 ± 0.01 | 0.35 ± 0.01 |
| $k_{cat}/K_m$ | 45,000 ± 7600 | 13,100 ± 2000 | 2400 ± 230 | 140 ± 20 | 320 ± 30 |
| 9-*cis*-retinaldehyde | | | | | |
| $K_m$ | 0.7 ± 0.1 | 0.7 ± 0.1 | 0.91 ± 0.12 | 0.5 ± 0.1 | 0.4 ± 0.1 |
| $k_{cat}$ | 0.9 ± 0.1 | 0.9 ± 0.1 | 0.27 ± 0.01 | 1.4 ± 0.1 | 0.7 ± 0.1 |
| $k_{cat}/K_m$ | 1300 ± 160 | 1300 ± 190 | 290 ± 40 | 2700 ± 790 | 1500 ± 170 |

Units: $K_m$ (mM with D,L-glyceraldehyde, μM with retinoids), $k_{cat}$ ($min^{-1}$), $k_{cat}/K_m$ ($mM^{-1}$ $min^{-1}$). Activities were determined as in Table 2.

We next studied the effect of substituting residue 304, Ser in 1B10, by Cys as found in 1B1 (Table 4). Again, no changes in glyceraldehyde kinetics were detected. Regarding the kinetics with all-*trans*-retinaldehyde, the S304C mutation had a strong effect on the $k_{cat}$ value comparable to that of the K125L mutation. Interestingly, when we studied the double mutation, there was an additive effect producing a 200-fold decrease in the $k_{cat}$ value, from 27 down to 0.12 $min^{-1}$, a value similar to that of 1B1. Thus, the joint contribution of Lys125 in loop A and of Ser304 in loop C could, in principle, explain the higher specificity of 1B10 for all-*trans*-retinaldehyde reduction. In contrast, no major effects were observed for single and double mutants on the kinetics with 9-*cis*-retinaldehyde. The $K_m$ values for both retinaldehyde substrates remained essentially unmodified by the mutations.

### 3.4. Molecular dynamics models of 1B1, 1B10 and 1B10 mutants complexed with NADP+ and all-trans-retinaldehyde

By inspecting the available three-dimensional structures of 1B1 and 1B10, we could not assess the combined role of residues 125 and 304. To this end we performed molecular dynamics on single and double mutant enzymes and compared the predicted structures with those of the wild-type complexes. Thus we run a total of four computer simulations of ternary complexes with extensive calculation times: 10 ns for each mutant and 4 ns for the wild-type simulation. The average structures obtained during the last 1 ns of the simulation are shown in Fig. 4A and B. In all simulations, atomic distances between the carbonyl group of all-*trans*-retinaldehyde and the catalytic and cofactor groups kept constant and correct for a productive catalysis to occur, although the position of the substrate appeared to be slightly different in each structure. Mutated residues were located far away from the anion binding site (catalytic site) and thus it is reasonable to assume that the activity decrease found in the single and double mutant enzymes is independent of the chemical step.

When exchanging Ser304 by Cys, some hydrogen bonds and hydrophobic interactions between loops A and C were broken (Fig. 4C and D). In fact, it has been reported that Ser304 is bridging a hydrogen-bond network between Gln114 (loop A) and main-chain oxygen of Val301 (loop C) in several ternary inhibitor complexes of 1B10 ([18,34], also Fig. 4C). In any case, loop A motion was quite different in the double mutant with respect to the single mutant (Fig. 4B). Somehow, these structural variations, which are exclusive to the double mutant, may have induced protein loop rearrangements and product–protein interaction changes. If the release of the product was the rate-limiting step [9], these changes affecting the product could be the reason for a lower $k_{cat}$ value in the double mutant. Despite the fact that, by making the double mutant, we tried to mimic the 1B1 structure, the explanation for decreased $k_{cat}$ values might be different in each complex, as suggested by the structural models. In the case of 1B1, Leu125 interacts hydrophobically with the substrate and may impair product release. In the case of the double mutant, loop rearrangement may also contribute to tighter binding of the product. Given the high variability of residues 303 and 304 in AKR1Bs and the results obtained with the double mutant, it seems that interactions between loops A and C could play a significant role in retinoid specificity. These features may be useful in order to design more selective 1B1 and 1B10 inhibitors.

### 3.5. Conclusions

In summary, the human genome contains three genes from the *AKR1B* subfamily *(1B1*, *1B10*, and *1B15*), while murine and rat genomes have four genes each. Phylogenetic and enzymatic activity analyses revealed that *1B10* gene orthologs cannot be unambiguously assigned. Differently from any other member from the mammalian AKR1B subfamily, human 1B10 is somewhat unique in having high all-*trans*-retinaldehyde reductase activity, indicating that gene function was not evolutionarily conserved within mammals. In particular, rat AKR1B10, here renamed as AKR1B17, has low activity with retinoids, supporting the fact that the two enzymes are neither functionally equivalent nor true orthologs. The high sequence identity between 1B10 and 1B15 warrants investigating whether 1B15 conserves high substrate specificity for retinoids.

Lys125, present in 1B10 protein, is also found in low-retinoid activity enzymes, which indicates that this is not the only structural determinant for high retinaldehyde reductase activity. In fact, here we have shown that Lys125 (loop A) and Ser304 (loop C), the latter being unique to 1B10 and chicken 1B12 (also a highly active retinaldehyde reductase [38]), are major structural determinants for all-*trans*-retinaldehyde specificity of 1B10, as assessed by site-directed mutagenesis and molecular dynamics.

## Conflict of interest

The authors declare that there are no conflicts of interest.

## Acknowledgements

We thank Professor T. Geoffrey Flynn (Department of Biochemistry, Queen's University, Kingston, Ontario, Canada) for his support. We wish to acknowledge the assistance of Terry Griest and Theresa Harter (Department of Ophthalmology, Washington University) toward the identification and characterization of novel aldo–keto reductases. We acknowledge the computer support, technical expertise, and assistance provided by the Barcelona Supercomputing Center-Centro Nacional de Supercomputación. This work was supported by grants from Dirección General de Investigación (BFU2008-02945 and FIS2008-03845), Generalitat de Catalunya (2009SGR795 and 2009SGR1309) and by NIH grant EY 05856. A.A. thanks the Spanish Ministry of Education for an FPU predoctoral fellowship.

## References

[1] Y. Jin, T.M. Penning, Aldo–keto reductases and bioactivation/detoxication, Annu. Rev. Pharmacol. Toxicol. 47 (2007) 263–292.
[2] J.M. Jez, M.J. Bennett, B.P. Schlegel, M. Lewis, T.M. Penning, Comparative anatomy of the aldo–keto reductase superfamily, Biochem. J. 326 (1997) 625–636.
[3] J.M. Jez, T.G. Flynn, T.M. Penning, A new nomenclature for the aldo–keto reductase superfamily, Biochem. Pharmacol. 54 (1997) 639–647.
[4] C. Yabe-Nishimura, Aldose reductase in glucose toxicity: a potential target for the prevention of diabetic complications, Pharmacol. Rev. 50 (1998) 21–33.
[5] O. Gallego, O.V. Belyaeva, S. Porté, F.X. Ruiz, A.V. Stetsenko, E.V. Shabrova, N.V. Kostereva, J. Farrés, X. Parés, N.Y. Kedishvili, Comparative functional analysis of human medium-chain dehydrogenases, short-chain dehydrogenases/reductases and aldo–keto reductases with retinoids, Biochem. J. 399 (2006) 101–109.
[6] S. Fukumoto, N. Yamauchi, H. Moriguchi, Y. Hippo, A. Watanabe, J. Shibahara, H. Taniguchi, S. Ishikawa, H. Ito, S. Yamamoto, H. Iwanari, M. Hironaka, Y. Ishikawa, T. Niki, Y. Sohara, T. Kodama, M. Nishimura, M. Fukayama, H. Dosaka-Akita, H. Aburatani, Overexpression of the aldo–keto reductase family protein AKR1B10 is highly correlated with smokers' non-small cell lung carcinomas, Clin. Cancer Res. 11 (2005) 1776–1785.
[7] T.M. Penning, AKR1B10: a new diagnostic marker of non-small cell lung carcinoma in smokers, Clin. Cancer Res. 11 (2005) 1687–1690.
[8] A.M. Quinn, R.G. Harvey, T.M. Penning, Oxidation of PAH trans-dihydrodiols by human aldo–keto reductase AKR1B10, Chem. Res. Toxicol. 21 (2008) 2207–2215.
[9] F.X. Ruiz, O. Gallego, A. Ardèvol, A. Moro, M. Domínguez, S. Álvarez, R. Álvarez, A.R. de Lera, C. Rovira, I. Fita, X. Parés, J. Farrés, Aldo–keto reductases from the AKR1B subfamily: retinoid specificity and control of cellular retinoic acid levels, Chem. Biol. Interact. 178 (2009) 171–177.
[10] R. Satow, M. Shitashige, Y. Kanai, F. Takeshita, H. Ojima, T. Jigami, K. Honda, T. Kosuge, T. Ochiya, S. Hirohashi, T. Yamada, Combined functional genome survey of therapeutic targets for hepatocellular carcinoma, Clin. Cancer Res. 16 (2010) 2518–2528.
[11] R. Wang, G. Wang, M.J. Ricard, B. Ferris, Y. Strulovici-Barel, J. Salit, N.R. Hackett, L.J. Gudas, R.G. Crystal, Smoking-induced up-regulation of AKR1B10 expression in the airway epithelium of healthy individuals, Chest 138 (2010) 1402–1410.
[12] O.A. Barski, S.M. Tipparaju, A. Bhatnagar, The aldo–keto reductase superfamily and its role in drug metabolism and detoxification, Drug Metab. Rev. 40 (2008) 553–624.
[13] R.D. Mindnich, T.M. Penning, Aldo–keto reductase (AKR) superfamily: genomics and annotation, Hum. Genomics 3 (2009) 362–370.
[14] T. Gui, T. Tanimoto, Y. Kokai, C. Nishimura, Presence of a closely related subgroup in the aldo–ketoreductase family of the mouse, Eur. J. Biochem. 227 (1995) 448–453.
[15] E.A. Pailhoux, A. Martinez, G.M. Veyssiere, C.G. Jean, Androgen-dependent protein from mouse vas deferens. cDNA cloning and protein homology with the aldo–keto reductase superfamily, J. Biol. Chem. 265 (1990) 19932–19936.
[16] P.J. Donohue, G.F. Alberts, B.S. Hampton, J.A. Winkles, A delayed-early gene activated by fibroblast growth factor-1 encodes a protein related to aldose reductase, J. Biol. Chem. 269 (1994) 8604–8609.
[17] C. Graham, C. Szpirer, G. Levan, D. Carper, Characterization of the aldose reductase-encoding gene family in rat, Gene 107 (1991) 259–267.
[18] D.J. Hyndman, R. Takenoshita, N.L. Vera, S.C. Pang, T.G. Flynn, Cloning, sequencing, and enzymatic activity of an inducible aldo–keto reductase from Chinese hamster ovary cells, J. Biol. Chem. 272 (1997) 13286–13291.
[19] O. Gallego, F.X. Ruiz, A. Ardèvol, M. Domínguez, R. Álvarez, A.R. de Lera, C. Rovira, J. Farrés, I. Fita, X. Parés, Structural basis for the high all-*trans*-retinaldehyde reductase activity of the tumor marker AKR1B10, Proc. Natl. Acad. Sci. U.S.A. 104 (2007) 20764–20769.
[20] A. Dereeper, V. Guignon, G. Blanc, S. Audic, S. Buffet, F. Chevenet, J.F. Dufayard, S. Guindon, V. Lefort, M. Lescot, J.M. Claverie, O. Gascuel, Phylogeny.fr: robust phylogenetic analysis for the non-specialist, Nucleic Acids Res. 36 (2008) W465–W469.
[21] J.D. Thompson, D.G. Higgins, T.J. Gibson, CLUSTAL W: improving the sensitivity of progressive multiple sequence alignment through sequence weighting, position-specific gap penalties and weight matrix choice, Nucleic Acids Res. 22 (1994) 4673–4680.
[22] M. Spite, S.P. Baba, Y. Ahmed, O.A. Barski, K. Nijhawan, J.M. Petrash, A. Bhatnagar, S. Srivastava, Substrate specificity and catalytic efficiency of aldo–keto reductases with phospholipid aldehydes, Biochem. J. 405 (2007) 95–105.
[23] B. Crosas, D.J. Hyndman, O. Gallego, S. Martras, X. Parés, T.G. Flynn, J. Farrés, Human aldose reductase and human small intestine aldose reductase are efficient retinal reductases: consequences for retinoid metabolism, Biochem. J. 373 (2003) 973–979.
[24] W.D. Cornell, P. Cieplak, C.I. Bayly, I.R. Gould, K.M. Merz, D.M. Ferguson, D.C. Spellmeyer, T. Fox, J.W. Caldwell, P.A. Kollman, A second generation force field for the simulation of proteins, nucleic acids, and organic molecules, J. Am. Chem. Soc. 118 (1996) 2309–12309, 117 (1995) 5179.
[25] D.A. Pearlman, D.A. Case, J.W. Caldwell, W.S. Ross, T.E. Cheatham, S. Debolt, D. Ferguson, G. Seibel, P. Kollman, Amber, a package of computer-programs for applying molecular mechanics, normal-mode analysis, molecular-dynamics and free-energy calculations to simulate the structural and energetic properties of molecules, Comput. Phys. Commun. 91 (1995) 1–41.
[26] S. Endo, T. Matsunaga, T. Kuragano, S. Ohno, Y. Kitade, K. Tajima, O. El-Kabbani, A. Hara, Properties and tissue distribution of a novel aldo–keto reductase encoding in a rat gene (Akr1b10), Arch. Biochem. Biophys. 503 (2010) 230–237.
[27] S.E. Old, S. Sato, P.F. Kador, D.A. Carper, In vitro expression of rat lens aldose reductase in *Escherichia coli*, Proc. Natl. Acad. Sci. U.S.A. 87 (1990) 4942–4945.
[28] S. Srivastava, T.M. Harter, A. Chandra, A. Bhatnagar, S.K. Srivastava, J.M. Petrash, Kinetic studies of FR-1, a growth factor-inducible aldo–keto reductase, Biochemistry 37 (1998) 12909–12917.
[29] D. Cao, S.T. Fan, S.S. Chung, Identification and characterization of a novel human aldose reductase-like gene, J. Biol. Chem. 273 (1998) 11429–11435.
[30] E.T. Lau, D. Cao, C. Lin, S.K. Chung, S.S. Chung, Tissue-specific expression of two aldose reductase-like genes in mice: abundant expression of mouse vas deferens protein and fibroblast growth factor-regulated protein in the adrenal gland, Biochem. J. 312 (1995) 609–615.
[31] A.M. Lefrancois-Martinez, C. Tournaire, A. Martinez, M. Berger, S. Daoudal, D. Tritsch, G. Veyssière, C. Jean, Product of side-chain cleavage of cholesterol, isocaproaldehyde, is an endogenous specific substrate of mouse vas deferens protein, an aldose reductase-like protein in adrenocortical cells, J. Biol. Chem. 274 (1999) 32875–32880.
[32] S. Endo, T. Matsunaga, H. Mamiya, A. Hara, Y. Kitade, K. Tajima, O. El-Kabbani, Characterization of a rat NADPH-dependent aldo–keto reductase (AKR1B13) induced by oxidative stress, Chem. Biol. Interact. 178 (2009) 151–157.
[33] S. Endo, T. Matsunaga, A. Fujita, K. Tajima, O. El-Kabbani, A. Hara, Rat aldose reductase-like protein (AKR1B14) efficiently reduces the lipid peroxidation product 4-oxo-2-nonenal, Biol. Pharm. Bull. 33 (2010) 1886–1890.
[34] S. Endo, T. Matsunaga, M. Soda, K. Tajima, H.T. Zhao, O. El-Kabbani, A. Hara, Selective inhibition of the tumor marker AKR1B10 by antiinflammatory N-phenylanthranilic acids and glycyrrhetic acid, Biol. Pharm. Bull. 33 (2010) 886–890.
[35] T. Matsunaga, S. Endo, M. Soda, H.T. Zhao, O. El-Kabbani, K. Tajima, A. Hara, Potent and selective inhibition of the tumor marker AKR1B10 by bisdemethoxycurcumin: probing the active site of the enzyme with molecular modeling and site-directed mutagenesis, Biochem. Biophys. Res. Commun. 389 (2009) 128–132.
[36] M. Verma, H.J. Martin, W. Haq, T.R. O'Connor, E. Maser, G.K. Balendiran, Inhibiting wild-type and C299S mutant AKR1B10; a homologue of aldose reductase upregulated in cancers, Eur. J. Pharmacol. 584 (2008) 213–221.
[37] H.T. Zhao, M. Soda, S. Endo, A. Hara, O. El-Kabbani, Selectivity determinants of inhibitor binding to the tumour marker human aldose reductase-like protein (AKR1B10) discovered from molecular docking and database screening, Eur. J. Med. Chem. 45 (2010) 4354–4357.
[38] B. Crosas, E. Cederlund, D. Torres, H. Jörnvall, J. Farrés, X. Parés, A vertebrate aldo–keto reductase active with retinoids and ethanol, J. Biol. Chem. 276 (2001) 19132–19140.